WORLD CONFERENCE ON TIMBER ENGINEERING 2025
BRISBANE, AUSTRALIA
Advancing Timber for the Future Built Environment

EVALUATION OF SEISMIC PERFORMANCE OF MID-RISE TIMBER BUILDINGS WITH SLIDING BASE SYSTEM

Ai Tomita[1], Yuji Miyazu[2]

ABSTRACT: This research proposes a sliding base system for mid-rise timber buildings and evaluates its seismic performance by time history seismic response analysis. The sliding base system is one of the base isolation systems, consisting of base concrete, sliding materials, and raft foundation. A case study building is a four-story timber frame building designed in accordance with the Japanese building standard act. A two-dimensional model for the case building was developed in OpenSees to perform time history response analysis. The sliding base was modelled by Coulomb friction elements to consider the variation of friction forces caused by pressure variation between the sliding elements. The coefficient of friction was set to 0.2 based on the mechanical property of the sliding material. The maximum story drift angle and acceleration response of the building subjected to severe earthquakes were significantly reduced by installing a sliding base system, indicating that the proposed system is effective to enhance seismic performance of mid-rise timber buildings. This result provides practitioners with alternative solutions for timber buildings constructed in earthquake-prone areas.

KEYWORDS: Mid-rise timber building, Sliding base system, Friction, Time history response analysis

1 – INTRODUCTION

In recent years, many mid-rise and high-rise timber buildings have been constructed around the world, even in earthquake-prone countries. In Japan, mid-rise timber buildings are attracting attention as an alternative to steel or concrete buildings; therefore, it is important to develop a practical method to enhance their seismic performance. Soda [1] proposed a sliding base system for wooden houses and evaluated the seismic performance through shaking table tests on a single story timber frame. The authors carried out shaking table tests on a two-story timber frame to confirm the effectiveness of the sliding base on multi-story timber bouldings [2]. Some research on sliding base isolation systems has been conducted not only in Japan but in other countries. The effects on the response acceleration of the superstructure and the sliding displacement of the base were evaluated a three-dimensional model of a single-story structure through linear dynamic analysis subject to multi-directional excitation [3]. This research proposes to introduce the sliding base system to a four-story timber frame building and evaluates the seismic response by time-history response analysis.

2 – METHOD

2.1 SLIDING BASE SYSTEM

Figures 1 and 2 illustrate the overview of the sliding base system. The sliding base consists of a sliding material and

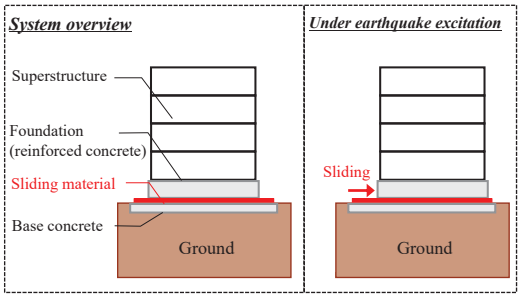

Figure 1. Overview of the sliding base system

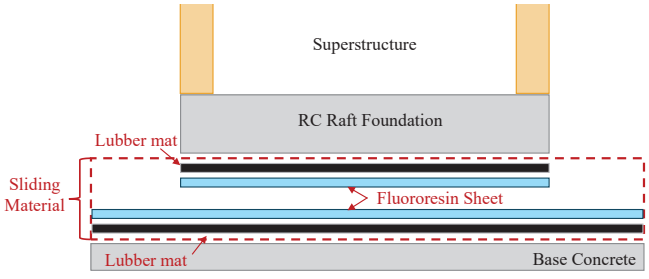

Figure 2. Configuration of the sliding base system

[1] Ai Tomita, Assistant Professor, Kyoto University, Dr. Eng., Uji-city, Japan, tomita.ai.2s@kyoto-u.ac.jp

[2] Yuji Miyazu, Associate Professor, Tokyo University of Science, Dr. Eng., Noda-city, Japan, miyazu@rs.tus.ac.jp

https://doi.org/10.52202/080513-0485

lubber mat inserted between the reinforced concrete (RC) raft foundation and the base concrete. A fluororesin sheet, which has a coefficient of friction of 0.2, was considered as the sliding material in this study. Since the friction coefficient between the fluororesin sheets is the lowest, sliding occurs between them during an earthquake. Our previous studies [1, 2] have confirmed that the sliding base system effectively reduced the seismic response of low-rise timber buildings.

2.2 NUMERICAL MODELLING AND TIME HISTORY ANALYSIS

Figure 3 shows a case study building used in this research [4]. Glued laminated timber is used for the beam and columns. Regarding the lateral-force resisting system, plywood panels are used in the longitudinal direction, while moment-resisting frames are used in the transverse direction. The aspect ratio of the building (H/B) was approximately 2.5. Figure 4 shows the overview of the transverse direction and the moment-resisting joints. Tensile bolt type joints are used for moment-resisting joint. Figure 5 illustrates a two-dimensional numerical model developed in OpenSees [5] for the transverse direction shown in Figure 4. Since the uplift at the foundation easily occurs in the transverse direction, only the transverse direction is modelled and the vertical displacement of the foundation caused by the overturning moment is evaluated. The mass of each floor was set at 4.53 t for the RC slab foundation, 3.25 t for the second floor, 3.20 t for the third

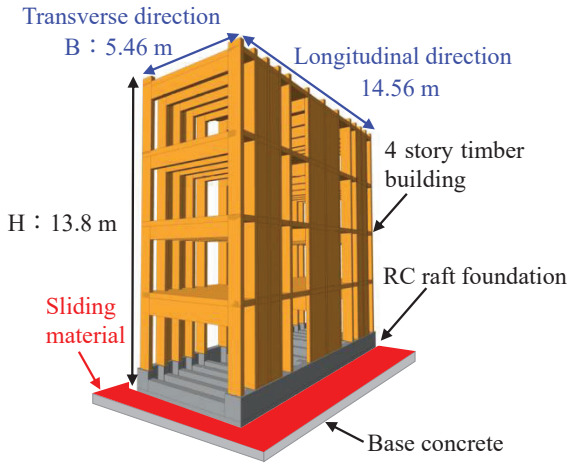

Figure 3. Four-story timber building with sliding base system

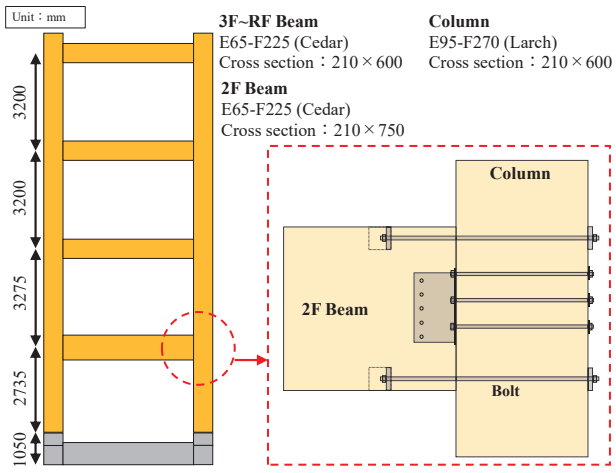

Figure 4. Overview of the transverse direction

Table 1. Cross-sectional area and mechanical properties of superstructure

Element	Young' modulus (N/mm^2)	Cross sectional area (mm^2)	Moment of inertia (mm^4)
Column	9.5×10^3	1.26×10^5	3.78×10^9
2F Beam	6.5×10^3	1.575×10^5	7.38×10^9
3F~RF Beam	6.5×10^3	1.26×10^5	3.78×10^9

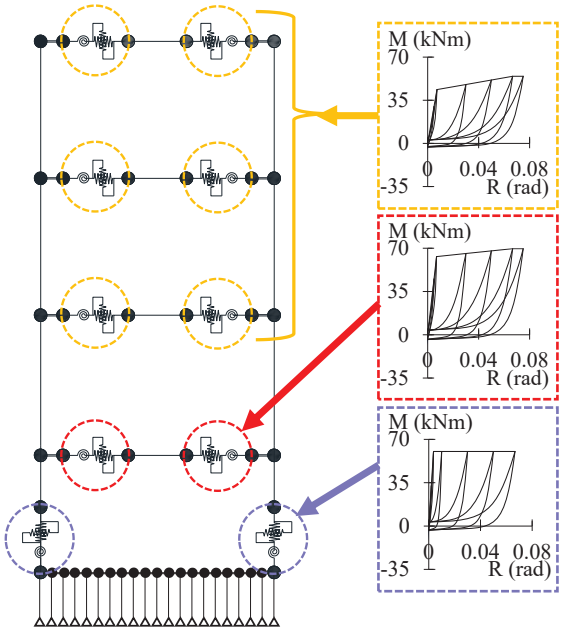

Figure 5. Overview of the analysis model

https://doi.org/10.52202/080513-0485

floor, 3.18 t for the fourth floor and 2.38 t for the roof floor. The mass at each node on the column was set to be half of the total mass of the floor. The numerical model of a building with the sliding base system (SB) was developed by the following four steps:

1) Modelling of the frame: The foundation and beam members were beam elements (elasticBeamColumn), and the columns were truss elements (truss). The cross-sectional area, moment of inertia of area, and Young's modulus of the elements are shown in Table 1.

2) Modelling of column-beam joints: The column-beam joints were modelled by a combination of shear springs, axial springs, and rotational springs. Elastic springs were used for the shear and axial springs, and the extended NCL model [6] (ENCL model) was used for the rotational spring. Equations (1) and (2) show the loading loop equation L_1 and unloading loop equation L_2 of the ENCL model.

$$L_1 = \mp Ax^4 + Bx|x|^{n1} + (1-B)x \pm A \quad (1)$$

$$L_2 = \pm Ax^4 + Bx|x|^{n2} + (1-B)x \mp A \quad (2)$$

Here, A represents the load intercept, B represents the slip gradient at the load intercept, and $n1$ and $n2$ represent the curve shape of the loop. Figure 5 shows the load-deformation relationship of each joint.

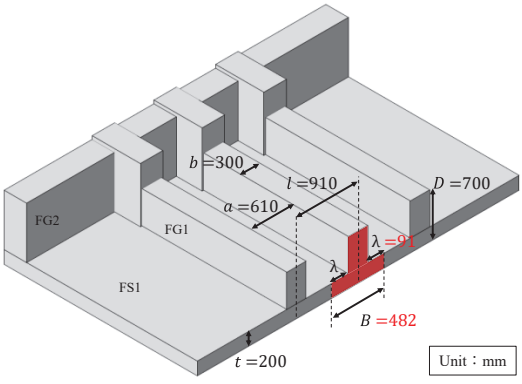

Figure 6. Overview of the RC foundation

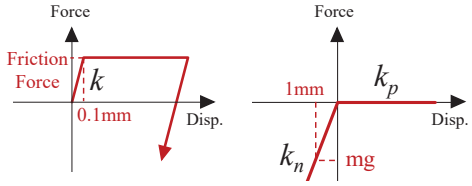

Figure 7. Load-deformation relationship of fSB element

3) Modelling of RC slab foundation: The cross-sectional area and moment of inertia of area were calculated using the effective width of the T-shaped member. As shown in Figure 6, the RC slab foundation has a T-shaped cross section, so λ was calculated using equation (3) to obtain the effective width B of the slab of the T-shaped cross section member, and the moment of inertia of area was calculated using equation (4).

Here, a (610 mm) is the distance between the sides of FG1, l (910 mm) is the distance between the centres of FG1, t (200 mm) is the height of FS1, D (700 mm) is

$$\lambda = \begin{cases} [a/l < 0.5] & \left(0.5 - \dfrac{0.6a}{l}\right)a \\ [a/l \geqq 0.5] & 0.1l \end{cases} \quad (3)$$

$$I = \frac{1}{3}\{Be_1^3 + be_2^3 - (B-b)(e_1-t)^3\} \quad (4)$$

$$e_1 = \frac{D^2 b + t^2(B-b)}{2\{Bt + b(D-t)\}}$$

$$e_2 = D - e_1$$

$$E_c = 3.35 \times 10^4 \times \left(\frac{\gamma}{24}\right)^2 \times \left(\frac{F_c}{60}\right)^{\frac{1}{3}} \quad (5)$$

Table 2. Cross-sectional area and mechanical properties of reinforced concrete

Young's modulus : E_c (N/mm²)	2.57×10⁴
Unit weight : γ (kN/m³)	24.5
Design basis strength : F_c (N/mm²)	24
Effective cross-sectional area of T-shaped (mm²)	2.464×10⁵
Area moment of inertia : I (mm⁴)	1.064×10¹⁰

Table 3. Total stiffness of fSB element

Horizontal	Vertical	
k (N/mm)	k_n (N/mm)	k_p (N/mm)
3.24×10⁵	1.62×10⁵	1.6×10

https://doi.org/10.52202/080513-0485

the height of the FG1, and b (300 mm) is the width of the FG1. The Young's modulus of concrete, E_c, was calculated using equation (5). γ is the unit weight and F_c is the design strength of concrete. Table 2 shows the values used in the calculation.

4) Modelling of the sliding foundation: The friction model was flatSliderBearing (hereinafter referred to as fSB) [7], which expresses Coulomb friction. This friction model assumes that frictional resistance is proportional to the normal force, independent of the contact area, and that the friction coefficient remains constant regardless of velocity. A fluororesin sheet was assumed as the sliding material, and its friction coefficient was set to 0.2. As shown in Figure 7 and Table 3, the stiffness of the horizontal and vertical linear springs in fSB was set sufficiently high while ensuring numerical integration stability. Specifically, the stiffness for the horizontal spring was defined such that the sliding load is reached with a deformation of 0.1 mm, and the compressive stiffness for the vertical spring was set to produce a deformation of 1 mm under the total weight of the model. The tensile stiffness of the vertical spring was set to a sufficiently small value (1/10,000 of the compressive stiffness) to simulate the uplift of the foundation. The beam element simulating the RC slab foundation was divided into 20 parts, and fSB was placed under each node.

To confirm the effect of the sliding base system on seismic performance, an analysis model with a fixed foundation (FB) and one with a sliding base system (SB) was also established. The 1st mode damping ratio of the superstructure is set to 1%, which is proportional to the initial stiffness. Damping of the sliding base was not applied in the horizontal direction, while it was set to 5% in the vertical direction. The first natural period was 0.742 s for the FB and 0.831 s for the SB.

Table 4. Input ground accelerations

Name (Abbreviation)	Max. Accel.
1940 Imperial Valley earthquake, El Centro NS Standardized to 50cm/s (El Centro Lv2)	5.10 m/s²
1952 Kern Country earthquake, Taft EW Standardized to 50 cm/s (Taft Lv2)	4.97 m/s²
1968 Tokachi earthquake, Hachinohe NS Standardized to 50 cm/s (Hacihnohe Lv2)	3.33 m/s²
1995 Kobe earthquake, JMA Kobe NS (KOBE)	8.18 m/s2

In order to investigate the effects of the aspect ratio of a building, numerical models with H/B=2.0 and 3.0 were also used in the time history analysis.

Four acceleration records listed in Table 4 were selected as input ground motions. KOBE wave, which was recorded during the 1995 Hyogoken-Nanbu Earthquake, and three ground motions commonly used in the seismic design of buildings in Japan were input. Since the sliding base system is designed to be effective for large earthquakes, the KOBE was used with its recorded acceleration. On the other hand, the other three ground motions were standardized to Level 2 (Lv2) with a velocity of 50 cm/s, the highest seismic intensity level considered in Japanese seismic design. Figure 8 shows the acceleration response spectrum with 5% damping.
Numerical integration was performed using the Newmark β method (β = 0.25), and the calculation time interval was 0.0001 seconds.

3 – RESULTS AND DISCUSSION

Figure 9 compares the maximum story drift angle and acceleration response between FB and SB. For SB, the story drift angle includes rotational deformations caused by the uplift of the foundation. The solid line in Figure 9 is the value including rotational deformation, while the dashed line is the value excluding rotational deformation. The sliding base system effectively reduces the response except for the maximum story drift angle at the fourth story during the Hachinohe Lv2 input. For FB, the deformation was less than 1/50 rad when a Level 2 earthquake motion was input. For KOBE excitation, the deformation was more than 1/30 rad. For SB, the response was less than FB, therefore the response reduction effect can be confirmed. Also, since the damage to the building was the shear deformation excluding rotational deformation of the foundation, the maximum story drift angle excluding rotational deformation was reduced to less than 1/100 rad for all

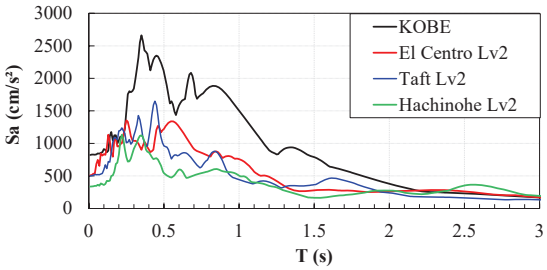

Figure 8. Acceleration response spectrum of the input ground accelerations (h = 5%)

https://doi.org/10.52202/080513-0485

ground accelerations. Figure 10 shows the ratio of SB and FB for the story drift angle and the maximum response acceleration. The ratio was almost equal to 1 for Hachinohe excitation because the response was small. Excluding the rotational deformation, the ratio was at most 0.6 for ground acceleration with a large response, and the response was reduced to about 0.3 times for KOBE excitation.

Figure 11 shows the time history of the vertical displacement, rotation angle, and sliding displacement of the sliding base. The positive value of the vertical displacement represents the uplift displacement of the foundation. The red line represents the vertical displacement at the left end of the foundation, while the blue line shows the vertical displacement at the right end of the foundation. The rotation angle is calculated by dividing the difference in vertical displacement between both ends by the foundation's width (5460 mm). The positive value of the sliding displacement indicates the sliding to the right from the original position, while the negative value

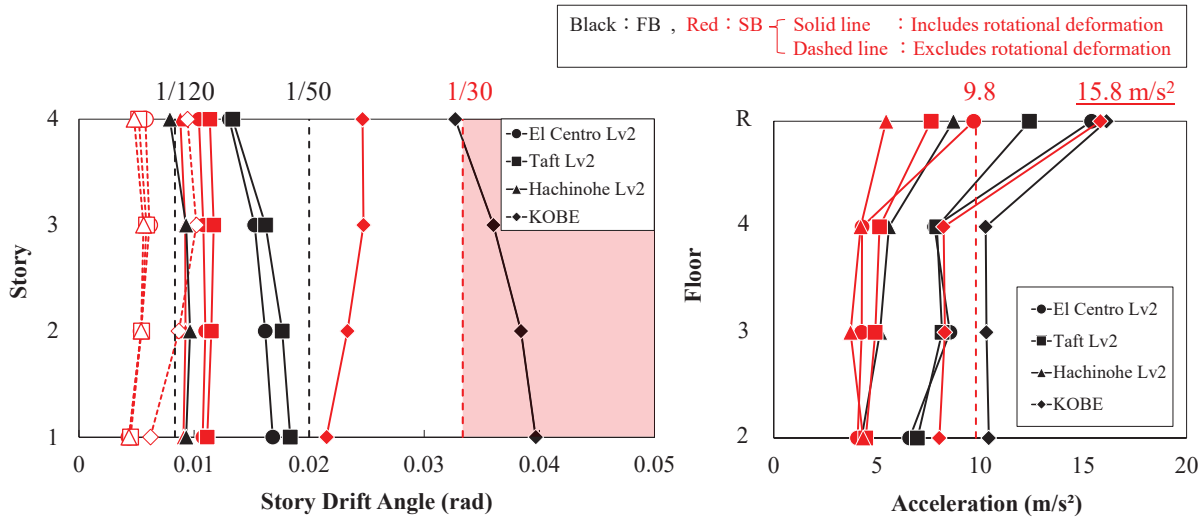

(a) *Story drift angle* (b) *Story drift angle*

Figure 9. Comparison of the maximum response of FB and SB

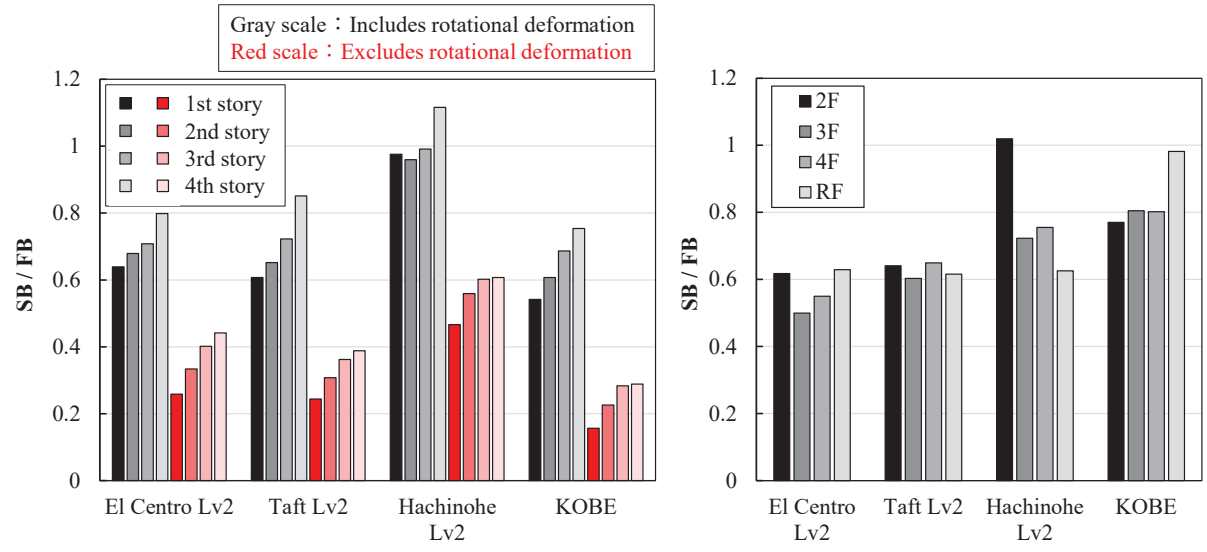

(a) *Story drift angle* (b) *Acceleration*

Figure 10. Ratio of maximum response of FB to SB

https://doi.org/10.52202/080513-0485

indicates the sliding to the left from the original position. It can be observed that vertical displacement occurs at the same time as the sliding for all ground motions. It can be observed that when the sliding occurs in the positive direction (to the right), the right end of the foundation remains in contact with the ground while the left end uplifts. Conversely, when the sliding occurs in the negative direction (to the left), the left end of the foundation remains in contact while the right end uplifts. The maximum vertical displacement is approximately 30 mm for Lv2 ground motions and around 100 mm for the KOBE ground motion. The maximum rotation angle due to the uplift of the foundation was approximately 0.01 rad under Lv2 ground motions and about 0.02 rad for the KOBE excitation.

Figure 12 shows the vertical displacements of each node in the foundation at the time when the vertical displacement at the foundation end is maximum, along with the compressive axial force in the fSB elements. It is observed that the vertical displacement is linearly distributed along the width of the raft foundation. It was found that the maximum compressive axial force at the foundation ends during uplift reaches approximately 40 kN in all cases, which is about five times the initial value.

Figure 13 shows a comparison of different aspect ratios when inputting KOBE. It shows the time history of the sliding displacement and rotation angle of the foundation, and the maximum story drift angle of the superstructure. The black line shows the results of an analysis model with the same aspect ratio as the target building. The blue line shows the results of a model with an aspect ratio of 2.0, which is wider than the original building. The red line shows the results of the model with the aspect ratio of 3.0, which is narrower than the original building. Figure 13(a) shows that the amount of sliding is greater in models with smaller aspect ratios. Figure 13(b) shows that the rotation angle of the foundation is also smaller when the aspect ratio is smaller, indicating that the small aspect ratio allows for stable sliding. Figure 13(c) shows that the inter-story deformation angle including rotational deformation of the foundation is larger in models with larger aspect ratios. On the other hand, when rotational deformation is excluded, it is suppressed to less than 1/100 rad in all models, confirming the response reduction effect of SB. It can be

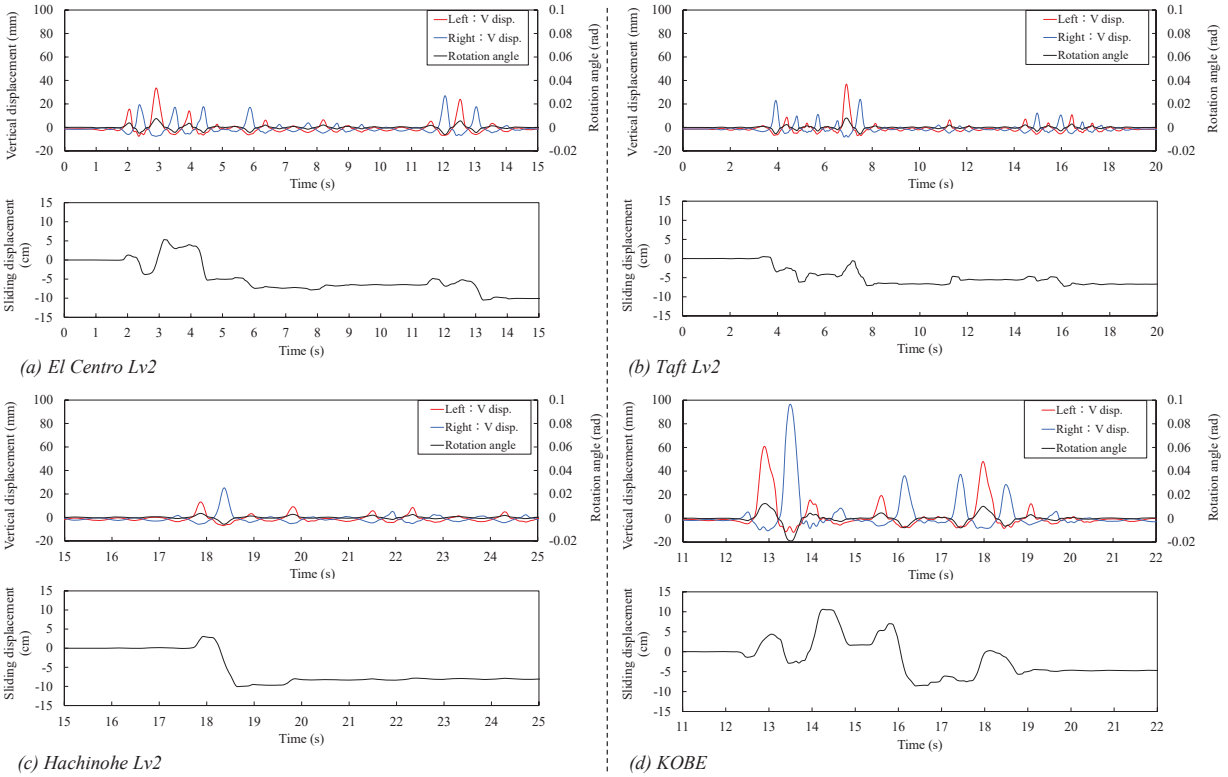

Figure 11. Time history of the vertical displacement, rotation angle, and sliding displacement of SB

https://doi.org/10.52202/080513-0485

seen that the small aspect ratio leads to a significant response reduction.

4 – CONCLUSIONS

This study examined the seismic performance of SB under various seismic inputs. As a result, it was confirmed that SB was effective in reducing seismic response under strong ground motion input, reducings the seismic response to approximately 0.3 times for KOBE excitation. By applying the sliding foundation structure, the maximum story drift angle of the superstructure was reduced to 1/100 rad or less. It was also confirmed that the response could be reduced to 1/100 rad by making the aspect ratio less than 3.0.

5 – REFERENCES

[1] S. Soda, Y. Miyazu "Seismic Response Control of Wooden House Placed on Sliding Base" In: Proceedings of the 9th U.S. National and 10th Canadian Conference on Earthquake Engineering, Paper No. 1508, 2010.

[2] A. Tomita, Y. Miyazu, T. Wakita, T. Tojo, T. Aoki, M. Nagano "Evaluation of Seismic Performance of Wooden Houses with Sliding Base by Full-scale Shaking Table Test" In: World Conference on Timber Engineering (WCTE2023), pp.2104-2110, 2023.

[3] H. Shakib, A. Fuladgar : Response of pure-friction sliding structures to three components of earthquake excitation, Computers & Structures 81, pp.189-196, 2003

[4] Mid-rise Large-scale Wooden Construction Research Association Design Support Information Database Ki, https://www.ki-ki.info/cont1/10.html, reference 2025. (in Japanese)

[5] PEER: OpenSees, http://opensees.berkeley.edu, reference 2024.

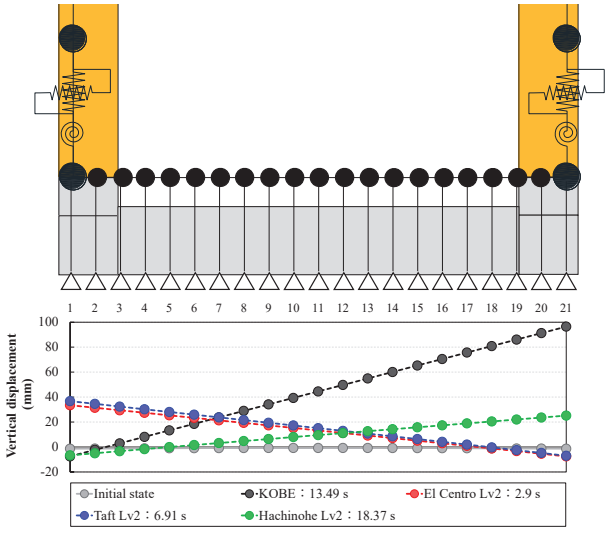

(a) Vertical displacement

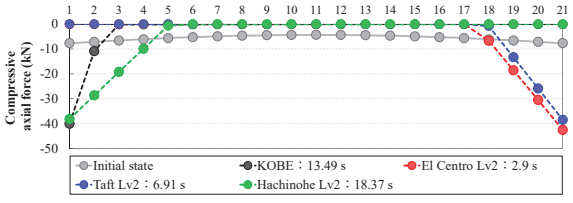

(b) Compressive axial force

Figure 12. Vertical displacement of the foundation and compressive axial force of the fSB elements

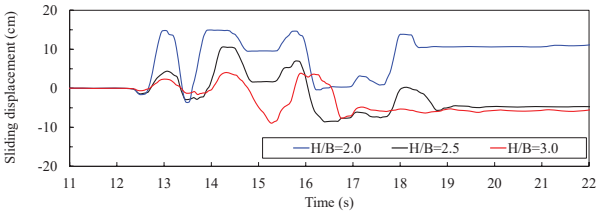

(a) Sliding displacement

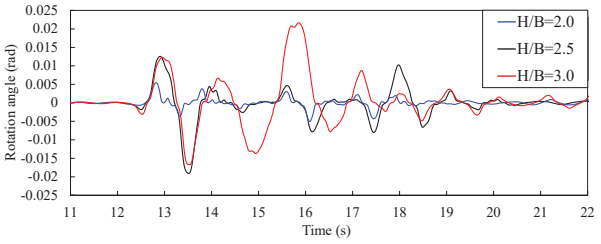

(b) Rotation angle

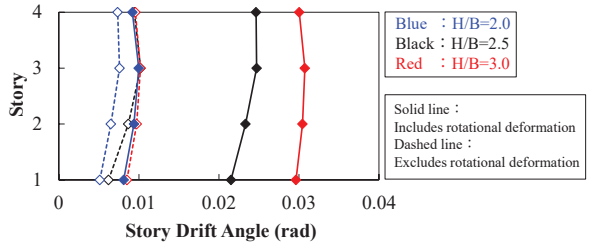

(c) Maximum story drift angle

Figure 13. Comparison of analysis models with different aspect ratios of superstructure (KOBE)

https://doi.org/10.52202/080513-0485

[6] H. Matsunaga, Y. Miyazu, S. Soda “A Universal Modelling Method for Wooden Shear/ Nonshear Walls” In: Journal of Structural and Construction Engineering, Vol. 74, pp.889-896, 2009. (in Japanese)

[7] OpenSees: flatSliderBearing, https://opensees.berkeley.edu/wiki/index.php/Flat_Slider_Bearing_Element, reference 2024.

https://doi.org/10.52202/080513-0485